ISBN: 978-3-95450-132-8 doi:10.18429/JACoW-IPAC2014-MOZA02

ADVANCED RF DESIGN AND TUNING METHODS OF RFQ FOR HIGH INTENSITY PROTON LINACS

Alain France, CEA-Irfu, Saclay, France

Abstract

This paper attempts to offer a survey of more recent developments in RF tuning of vane RFQs, and to show how tunability constraints are related to design. Vane RFQs are particularly well suited to high intensity proton acceleration, since they offer minimal RF power losses and best accelerating field accuracy. Four such vane-RFQs have been or are under development at CEA-Irfu, namely IPHI, Spiral2, Linac4 and ESS. Design and tuning of these RFQs are integrated in a common rigorous theoretical framework, leading to common design rationale and common measurement-processing and tuning algorithms.

INTRODUCTION AND THEORETICAL FRAMEWORK

The four vane-RFQs developed at Saclay are presented in Table 1. IPHI, a 6-meter long RFQ divided into three capacitively coupled segments, is now tuned [1]; commissioning is expected to start in 2014 Q3. Fabrication of the five Spiral2 1-meter modules is close to completion, with tuning operations starting in 2014 Q3. Linac4 RFQ is now operational [2], while ESS RFQ [3] is still under development.

Table 1: RFQ projects at CEA-Irfu

	IPHI	Spiral2	Linac4	ESS
location	CEA Saclay	GANIL Caen	CERN Geneva	ESS Lund
status	tuned	fab.	op.	dev.
F (MHz)	352.2	88.05	352.2	352.2
L (m)	6	5	3	4.5
I_B (mA)	100	5	80	62.5
duty cycle	CW	CW	7.5%	4%
W (MeV/u)	3	3	3	3.6
segments	3	1	1	1
modules	6 brazed	5 bolted	3 brazed	5 brazed
RF coupler	4 irises	4 loops	1 iris	2 loops
Tuning:				
slugs	96	40	32	60
RF ports	4	0	4	0
plates	5	0	0	0
Q rods sets	1	2	2	2
D rods sets	6	0	0	0
total	112	42	38	62

Specified resonance frequencies and inter-vane voltage functions of these RFQs are obtained via the careful adjustment of tuning devices, which may be slugs, thickness plates, rods, active RF ports or dummy RF ports, and generally a combination of these. Their number varies from 38 for Linac4 to 112 for IPHI, excluding any try-and-cut procedure. Note by the way that both design and tuning are inverse problems, where geometrical parameters are deduced from electromagnetic quantities. An ideal theoretical framework would then provide an invertible model of an arbitrary (i.e. imperfect) and tunable RFQ. Such a model should be (1) accurate, i.e. able to mimic results of exact 3D simulations and (2) fast enough to be usable in practical tuning operations. The loaded lossless 4-wire transmission line model (TLM), previously described in [4], has been consistently used for design and tuning in the four aforementioned projects. According to this model, the field maps in the RFQ axial region are assumed to be supported by a 4-wire system loaded by parallel impedances representing the RFQ quadrants. This system is characterized by a voltage 3-vector (since three cuts make the system of conductors simply connected); quadrupole (U_Q) and dipole (U_S,U_T) components of U are related to inter-electrode voltages $u_{1\ldots4}$ by

$$U_Q = (u_1-u_2+u_3-u_4)/4,\ U_S = (u_1-u_3)/2,\ U_T = (u_2-u_4)/2. \quad (1)$$

End and coupling-circuits (if any) are represented by arbitrary lossless reciprocal circuits, leading to the boundary conditions

$$\partial U(a)/\partial z = -s_a U(a)\,,\quad \partial U(b)/\partial z = -s_b U(b)\,,\quad \left|\begin{matrix}\partial U(z_i^-)/\partial z\\ \partial U(z_i^+)/\partial z\end{matrix}\right| = s_i \left|\begin{matrix}U(z_i^-)\\ U(z_i^+)\end{matrix}\right|, \quad (2)$$

in z = a,b (RFQ ends) and z = z_i (coupling-circuits). The RFQ is then represented by the eigen-value problem

$$\mathcal{L}\,U = \lambda U\,,\quad (\lambda = \omega^2/\nu^2), \quad (3)$$

where the operator $\mathcal{L}$ is defined for all vector functions satisfying the boundary conditions by

$$\mathcal{L}\,U = -C_Q^{-1}\frac{\partial}{\partial z}\left(C_Q\frac{\partial U}{\partial z}\right) + \nu^{-2}C^{-1}L_Q\,U, \quad (4)$$

where C_Q, L_Q are the capacitance (F/m) and inductance (H.m) matrixes, ω is the radian frequency and ν is the speed of light in the filling medium (air or vacuum). The operator $\mathcal{L}$ is linear unbounded and self-adjoint with linear bounded and compact inverse, hence has a pure point spectrum. Its eigen pairs may be distributed in the three Q, S and T subsets

$\{\omega_{Xi}, V_{Xi}(z) = |V_{Xi,Q}(z), V_{Xi,S}(z), V_{Xi,T}(z)|^t\}$, $X \in \{Q,S,T\}$.

Note that in the ideal case of a quaternary-symmetric RFQ, L_Q, C_Q are diagonal, and the only non-zero components of the eigen-functions are the $V_{Xi,X}(z)$.

The values of line parameters are determined in such a way both TLM and exact 2D/3D simulations yield identical results. The inductances and capacitances are calculated in short RFQ elements, each one corresponding to an accelerating "cell". In the ESS design (Fig. 1) vane-

ISBN: 978-3-95450-132-8 doi:10.18429/JACoW-IPAC2014-MOZA02

tip modulations have negligible effect on parallel capacitance (i.e. between adjacent vanes), but have a large impact on diagonal capacitance (i.e. between opposite vanes) hence on RFQ stability. The type of modulation is also important: the modulation derived from the 2-term potential expression induces much less detuning than the simpler sine modulation, and should be preferred (Fig. 2).

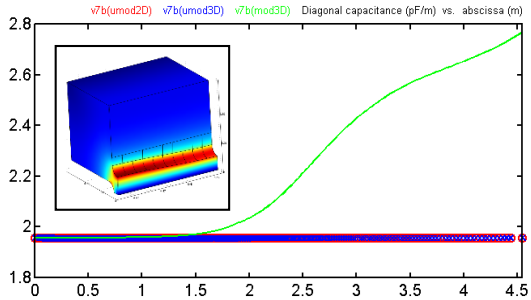

Figure 1: ESS diagonal capacitance, in three cases: un-modulated 2D calculation (red), un-modulated 3D (blue) and modulated 3D (green). One computation cell is shown in insert.

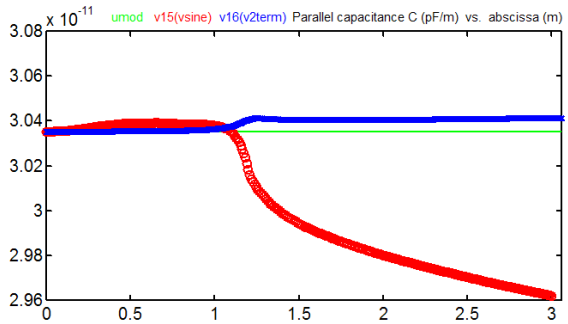

Figure 2: Linac4 parallel capacitance, in three cases: un-modulated 2D calculation (green), sine modulation (red) and modulation derived from 2-term potential (blue).

END & COUPLING CIRCUITS TUNING

End and coupling circuits must be tuned in such a way the specified voltage function V(z) could belong to the Q subset of problem (3) eigen-functions. Constraints resulting on end s-matrixes are $s_{QQ} = -(1/V)\,\partial V/\partial z$ at RFQ input and $s_{QQ} = +(1/V)\,\partial V/\partial z$ at output. The QQ block of a coupling-circuit s-matrix reads

$$\begin{vmatrix} s_e^- + s_c & -s_c \\ -s_c & s_e^+ + s_c \end{vmatrix}, \qquad (5)$$

where the coupling coefficient $s_c = (\omega/v)^2 C_c/4C$ is directly related to the coupling capacitance C_c, and where the $s_e^{\pm}$ are the even-mode coefficients. The conditions

$$s_{\Delta\Sigma} = -(s_e^- + s_e^+)/2 = 0 \quad \text{(matching)} \qquad (6)$$

$$s_{\Sigma\Sigma} = (s_e^- - s_e^+)/2 = (1/V)\,\partial V/\partial z \quad \text{(tuning)} \qquad (7)$$

ensure that the voltage eigen-function is continuous (matching) and has the right slope (tuning) across the coupling-circuit mid-plane. Specified values of s_{QQ}, s_c, etc. are derived from the 3D simulation of a short element of RFQ (typically 30 to 50 cm long), in such a way the TLM applied to the same element yields the same eigen-spectrum. Measured values are obtained with the excitations set method: M linearly independent pairs {U, $\partial U/\partial z$} satisfying $\partial U/\partial z = s\,U$ are used to estimate all coefficients of s. These excitations are obtained with M preset tuner positioning at some distance from boundary. Using M = 5 for end-circuits and M = 11 for coupling-circuits usually yields adequate accuracy. Results obtained for IPHI and Linac4 RFQ are reported in Table 2; "tuning" values are measured with aluminum tuning devices (as the ones shown in Fig. 3), and "tuned" values with machined copper parts.

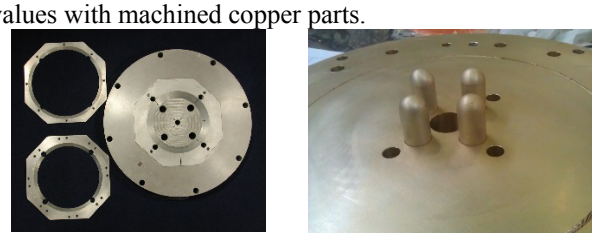

Figure 3: Example of tuning devices: adjustable thickness plates (left) and quadrupole rods set (right).

Table 2: IPHI and Linac4 Boundary Conditions Tuning. All values are in m^{-1}, unless otherwise specified.

		expected	tuning (Al)	tuned (Cu)
IPHI				
input	s_{QQ}	0.0	$-5.46\ 10^{-3}$	$-3.04\ 10^{-2}$
	$\sigma(s_{QQ})$		$1.55\ 10^{-2}$	$3.01\ 10^{-2}$
cc1	$s_{\Sigma\Sigma}$	$+7.91\ 10^{-2}$	$+7.33\ 10^{-2}$	$+9.45\ 10^{-2}$
	$s_{\Delta\Sigma}$	0.0	$+9.29\ 10^{-3}$	$-9.59\ 10^{-2}$
	C_{c1}	1.1 pF	0.71 pF	0.53 pF
cc2	$s_{\Sigma\Sigma}$	$1.30\ 10^{-1}$	$+1.07\ 10^{-1}$	$+1.20\ 10^{-1}$
	$s_{\Delta\Sigma}$	0.0	$+1.82\ 10^{-2}$	$+2.39\ 10^{-3}$
	C_{c2}	1.1 pF	0.93 pF	0.95 pF
output	s_{QQ}	$+2.11\ 10^{-2}$	n/a	$+2.85\ 10^{-2}$
	$\sigma(s_{QQ})$		n/a	$1.67\ 10^{-2}$
LINAC4				
input	s_{QQ}	0.0	$+2.78\ 10^{-2}$	$+6.26\ 10^{-2}$
	$\sigma(s_{QQ})$		$7.00\ 10^{-2}$	$2.41\ 10^{-2}$
output	s_{QQ}	0.0	n/a	$-7.67\ 10^{-2}$
	$\sigma(s_{QQ})$		n/a	$2.97\ 10^{-2}$

The general accuracy on s-matrixes coefficients is a few $10^{-2}\ m^{-1}$, leading to voltage errors of a few 10^{-3} between the boundary and the closer tuner. All boundaries appear to be correctly tuned, with three notable exceptions: (1) the first coupling-circuit of IPHI suffers from low coupling capacitance, likely resulting from inaccuracies in 20-year old computer simulations; (2) the same coupling-circuit also suffers from a slight mismatch, in fact due to mechanical instability from uncertain origin; and (3) the Linac4 RFQ end-circuits are purportedly slightly detuned for stability reasons cited in the next paragraph.

STABILITY DESIGN & MEASUREMENT

The "stability" of a RFQ measures its sensitivity to perturbations during operation. These perturbations

ISBN: 978-3-95450-132-8 doi:10.18429/JACoW-IPAC2014-MOZA02

primarily result from thermal deformations, and translate into RFQ inductance and capacitance perturbations. First-order perturbation analysis of the TLM reveals dual bases for parameter perturbation functions and resulting voltage perturbation functions. For example, capacitance perturbations are described in a $\{C_{QQ}, C_{SQ}, C_{TQ}\}$ basis, in correspondence with the $\{U_Q, U_S, U_T\}$ basis.

$$C_1 = C_{QQ} + C_{SQ} + C_{SSTT}, \quad C_3 = C_{QQ} - C_{SQ} + C_{SSTT},$$
$$C_2 = C_{QQ} - C_{TQ} - C_{SSTT}, \quad C_4 = C_{QQ} + C_{TQ} - C_{SSTT},$$

The RFQ sensitivity to quadrupole-like perturbations is then described by the impulse error function $h_{Qn,Q}$

$$\frac{\Delta V_{Qn,Q}(z)}{V_{Qn,Q}(z)} = h_{Qn,Q}(z, z_0)\frac{\Delta c_{QQ}}{C(z_0)} \qquad (8)$$

which relates a Dirac-like perturbation with mass $\Delta c_{QQ}/C$ located in z_0, to the resulting voltage relative perturbation $\Delta V_{Qn,Q}/V_{Qn,Q}$. Similar relations define dipole-like impulse error functions $h_{Qn,S}$ and $h_{Qn,T}$ (equal to a common $h_{Qn,S/T}$ function in symmetric designs). Finally, RFQ designs and/or realizations may be compared with the norms

$$\|h_{Qn,X}\| = \sup_{z\in\Omega}\sup_{z_0\in\Omega}|h_{Qn,X}(z, z_0)|, \quad X\in\{Q,S,T\},$$

which play the roles of figures of merit. The $h_{Qn,X}$ functions are infinite series whose terms are inversely proportional to eigen-value differences $\lambda_{Qn} - \lambda_{Xi}$, i.e. quadratic frequency separation (QFS) $(f_{Qn})^2 - (f_{Xi})^2$. Impulse error functions are infinite each time an eigen-value coincide with the accelerating mode eigen-value.

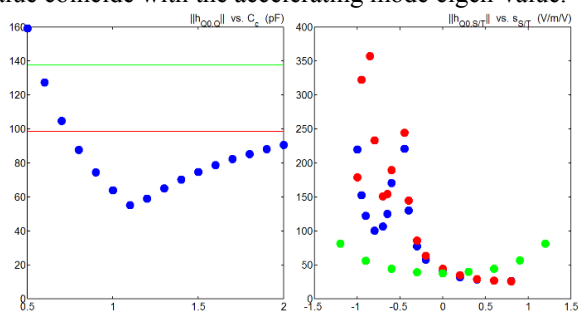

Figure 4: IPHI stability. Impulse error function norms $\|h_{Qn,Q}\|$ (left) and $\|h_{Qn,S/T}\|$ (right) are plotted in three cases: un-segmented design (green), segmented design (blue), and measured (red).

The norm $\|h_{Qn,Q}\|$ depends on RFQ length and on the accelerating mode (Q_0) eigen-value only for a single-segment RFQ, and can be modified only by segmentation; a rather sharp optimum is then usually found for the value of coupling capacitance(s), as shown for IPHI in Fig. 4 (left). Note that the too low value of C_{c1} increases the sensitivity to quadrupole-like perturbations by a factor 2. Once segment lengths and coupling capacitances have been chosen, the norms $\|h_{Qn,S/T}\|$ depend only on s-matrix coefficients pertinent to dipole modes: s_{SS}, s_{TT}, $s_{Se}^{\pm}$, $s_{Te}^{\pm}$. $\|h_{Qn,S/T}\|$ is plotted vs. their (assumed) common value $s_{S/T}$ in Fig. 4 (right) and is seen to present a minimum for $s_{S/T} = 0 \sim 0.5$. This value is reached thanks to dipole rods with adequate length (about 0.2 free-space wavelength). The sensitivities of unsegmented and segmented designs to dipole-like perturbations are found to be equal. Eigen-frequencies and QFS of modes closer to the accelerating mode are reported in Table 3.

Table 3: IPHI eigen-frequencies and QFS (between brackets), in MHz.

mode	spec	prior to slug tuning	after slug tuning
$\mathbf{Q_{0-1-0}}$	348.18 [–42.0]	349.55 [–25.1]	351.25 [–24.5]
$\mathbf{Q_{0+0+0}}$	350.71 [0.0]	350.45 [0.0]	352.10 [0.0]
$\mathbf{Q_{1-1-1}}$	353.69 [+47.8]	354.65 [+54.4]	356.40 [+55.2]
$\mathbf{D_{1+1+1}}$	347.67 [–46.1]	348.10 [–40.5]	349.30 [–44.3]
$\mathbf{Q_{0+0+0}}$	350.71 [0.0]	350.45 [0.0]	352.10 [0.0]
$\mathbf{D_{2-2-2}}$	363.16 [+94.3]	362.60 [+93.1]	364.30 [+93.5]

The lengths of the Linac4, Spiral2 and ESS RFQs have been chosen in such a way they satisfy beam dynamics constraints while leading to $s_{S/T}$ values realizable without dipole rods. A detailed description of Linac4 tuning is given in [5]; a discrepancy has been found between calculated and measured $s_{S/T}$ values vs. length of quadrupole rods, both at input and output plates. A slight detuning of the rods has been used to recover acceptable sensitivity to dipole-like perturbations.

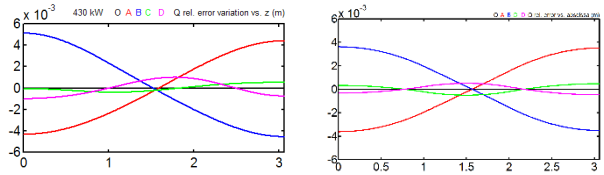

Figure 5: sensitivity of Linac4 voltage to temperatures of RFQ modules. Left: measured, right: expected.

The sensitivity of Linac4 voltage to temperature variations has been quantified thanks to monitoring pickups located in 16 copper slugs. An appropriate sampling theory is used to reconstruct continuous inter-vane voltage functions. Temperatures $T_{1,2,3}$ of the three RFQ modules can be controlled independently with a 0.1°C accuracy. In the reference "O" case, $T_1 = T_2 = T_3 =$ 26°C; the RFQ is operated at its 430 kW nominal RF power. Pulse duration and repetition interval are PD = 250 µs, PRI = 1.2 s. Four variations are defined as

"A" 25.5 – 26.0 – 26.5, "C" 26.5 – 26.0 – 26.5,
"B" 26.5 – 26.0 – 25.5, "D" 25.5 – 26.0 – 25.5;

reconstructed voltage relative variations are plotted in Fig. 5 (left). RFQ deformation is primarily thermal expansion at such a low duty factor; expected voltage variations then calculated by the TLM model are plotted in Fig. 5 (right). The agreement with measured data clearly demonstrates that the TLM is able to accurately capture the RFQ behaviour, and more generally, sustains the whole design procedure [4].

VOLTAGE AND FREQUENCY TUNING

Voltage and frequency tuning is realized thanks to slugs regularly distributed along each RFQ quadrant. These slugs produce discrete perturbations of quadrant inductances, which in turn produce voltage perturbations. These should cancel voltage errors pre-existing in the un-tuned RFQ.

ISBN: 978-3-95450-132-8 doi:10.18429/JACoW-IPAC2014-MOZA02

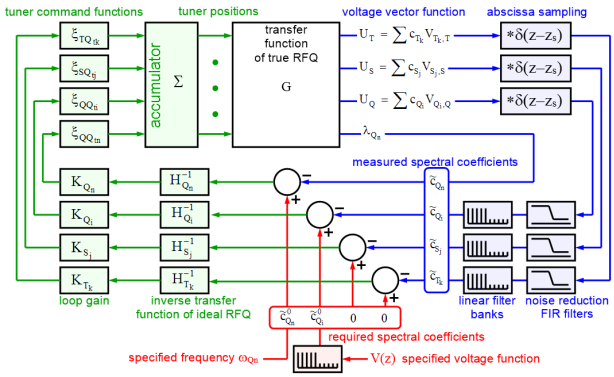

Fig. 6: Tuning algorithm.

This principle is implemented in a closed-loop control-command tuning algorithm based on dual spectral decompositions of inductance and voltage perturbations (Fig. 6). Note that the calculation of spectral coefficients and inductance basis functions requires the knowledge of boundary conditions, which should have been tuned in first place.

The tuning loop exhibits some interesting features, all resulting from the fact it is equivalent to the fixed-point iteration of the operator $A = I - G\,K\,H^{-1}$ (where G is the true RFQ transfer matrix, K is the gain matrix and H is the ideal RFQ transfer matrix, see Fig. 6). The loop is unbiased. It converges if and only if A is a contraction, a condition here satisfied if and only if eigen-modes are identically sorted for the true and ideal RFQs according to eigen-value order. Convergence is monotonic if A is diagonal, but may be non-monotonic otherwise.

Proper operation of the algorithm requires many additional conditions to be satisfied. Acquired field samples should reside far enough from local perturbations (as tuners or vacuum ports), while being sufficiently regularly spaced in such a way reconstructing filters are not singular, and also free from aliasing in the set of tuned spectral components. Slug tuners should be sufficiently regularly distributed in such a way their spectral transmittance is free from aliasing; large RF ports (as iris couplers of IPHI and Linac4) should be included in the tuner set. A close-to-ideal distribution of field samples and tuners is depicted in Fig. 7.

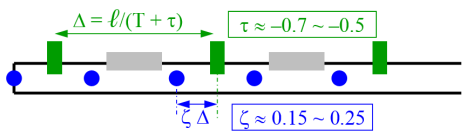

Figure 7: Close-to-optimum distribution of tuners (green), field samples (blue) and other perturbations (grey).

Tuner "efficiency" is represented by the slope dL/dh of inductance vs. slug position h; it is usually constant over a large range, as in Fig. 8 (left). The elaboration of tuner position range specification starts with the transformation of fabrication tolerances (applying to vane-tip radius and centre of curvature, for instance) into inter-vane capacitance errors. The resulting volume is generally a zonohedron (a particular class of polyhedra), as in Fig. 8 (right). The TLM and its first-order perturbation analysis are then particularly well suited to the calculation of tuner position limits, using linear programming (Danzig's simplex algorithm).

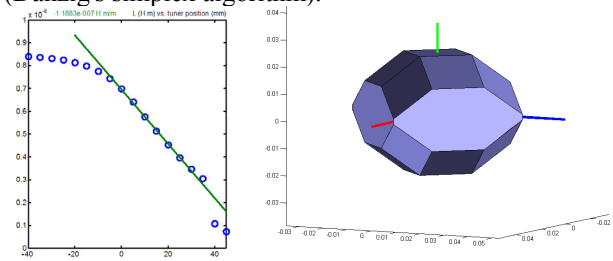

Figure 8: Linac4 example. Left: tuner inductance vs. tuner position (>0 inside RFQ). Right: capacitance polyhedron in C_{QQ}, C_{SQ}, C_{TQ} axes (resp. in green, red, blue).

Table 4: IPHI and Linac4 Voltage Tuning Summary

IPHI			
voltage peak relative errors (%):	**Q**	**S**	**T**
dummy RF ports, un-tuned	90	17.6	14.5
adjustable slugs, RF ports, tuned	0.78	0.28	0.63
copper slugs	3.97	1.32	2.07
tuner positions (mm): specified	+1.0 / +19.0		
specified, with safety margin	–5.0 / +25.0		
tuned RFQ	–1.7 / +12.5		
LINAC4			
voltage peak relative errors (%):	**Q**	**S**	**T**
dummy RF port, un-tuned	5.55	5.53	7.19
adjustable slugs, RF port, tuned	0.70	1.48	3.07
copper slugs	0.63	3.45	2.29
tuner positions (mm): specified	–4.0 / +30.0		
tuned RFQ	+9.0 / +12.1		

Voltage tuning results are reported in Table 4. Linac4 RFQ uses only a small fraction of its specified range, as its capacitance errors [5] are well within the specified polyhedron. A general increase of voltage errors occurs as adjustable slugs are replaced by their machined counterparts; these errors are essentially random, and would require several tuning iterations for cancellation. The large increase of IPHI voltage Q-component however has been traced back to a structural instability of coupling circuit #1, either due to the RFQ body itself or its support.

RF POWER COUPLING

RF power is coupled to IPHI and Linac4 RFQs by iris couplers (Fig. 9) matched to WR2300 feeders by quarter-wave impedance transformers made with ridged waveguide. Diameter of circular openings at both iris ends is adjusted to achieve desired coupling coefficient, and position of the whole assembly to minimize voltage perturbation [1]; losses in final full copper RFQ have to be anticipated at that point. Spiral2 and ESS will be fed via loops specially designed to induce negligible voltage perturbation: they don't need to be included in the set of tuners, and coupling coefficient of the full copper RFQ may be adjusted. Loops also present less losses then irises, and are a preferred option.

ISBN: 978-3-95450-132-8 doi:10.18429/JACoW-IPAC2014-MOZA02

Figure 9: IPHI (left) and Linac4 (right) iris couplers.

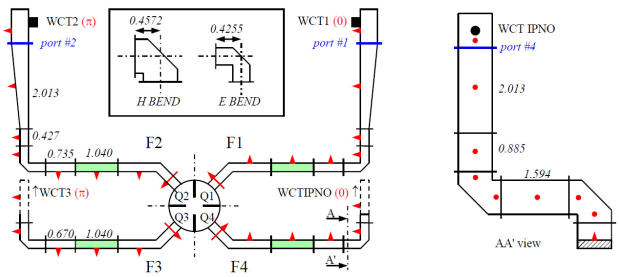

Figure 10: IPHI measurement setup. Vacuum windows are located in green sections. Voltage convention is shown with red arrows, and feeder inputs with blue lines.

From an RF point of view, IPHI is a 4-port circuit, fully characterized by its 4×4 scattering matrix. The measurement set-up is sketched in Fig. 10; the RFQ is under vacuum. S-matrixes of measurement cables and WCTs are measured, and a scattering matrix S, defined at WR2300 feeder inputs, is de-embedded (Fig. 11). Coefficients of transmission to adjacent quadrant may be accurately represented by

$$s_{i,j}(\omega) \approx \frac{\sqrt{\beta_i\beta_j}}{1+\beta}\left(1+e^{j\alpha(\omega)}\right)\zeta_{i,j}(\omega), \qquad (9)$$

and coefficients of transmission to opposite quadrant by

$$s_{i,j}(\omega) \approx -\left(\frac{\sqrt{\beta_i\beta_j}}{1+\beta}\left(1+e^{j\alpha(\omega)}\right)+j\sqrt{\beta_i\beta_j}H(\omega)\right)\zeta_{i,j}(\omega); \qquad (10)$$

they are fully determined by the polar angle $\alpha(\omega)$, the offset function $H(\omega)$, the phasors $\zeta_{i,j} = \zeta_i\zeta_j$ representing propagation in feeder lines, and the partial coupling coefficients $\beta_{1\ldots4}$. All these quantities are easily extracted from measured S using inverse projections in the complex plane; resonance frequency ω_0 and unloaded quality factor Q_0 are derived from $\alpha(\omega)$.

The RFQ is matched to its transmitter(s) if the excitation 4-vector is an eigen-vector e_1 of S^*S corresponding to its smallest eigenvalue λ_1; coupling bandwidth is a comfortable 100 kHz (Fig. 11). Interestingly, ω_0, Q_0 and $\beta_{1\ldots4}$ may be also derived from the eigen-pair $\{\lambda_1, e_1\}$. Both methods yield quite close results as shown in Table 5; corrected β_is take into account quadrant voltage tuning errors.

Operational parameters of IPHI and Linac4 are reported in Table 6; power dissipated in copper P_{Cu} is deduced from realized Q_0 and theoretical stored energy. Ideal β is deduced from P_{Cu} and beam power P_B, and Γ^2 is the expected power reflection coefficient under operation with beam. Realized Q_0s are quite close as expected for RFQs sharing the same technology. The slightly low value of IPHI realized β likely results from deformation of quarter-wave transformers during braze.

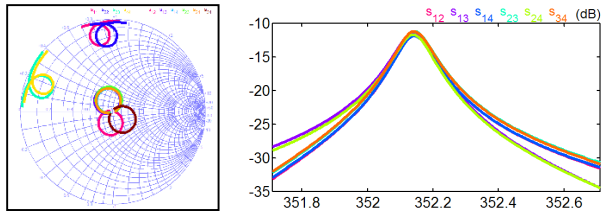

Figure 11: Measured S-matrix plotted in the complex plane (left) and $s_{i,j}$ amplitudes (in right). The two families of transmission coefficients are clearly visible.

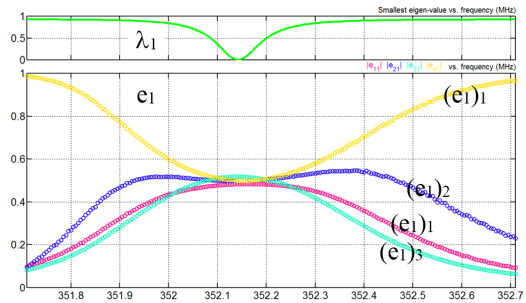

Figure 12: Smallest eigen-value of S^*S and amplitudes of associated eigen-vector components.

Table 5: IPHI RF Coupling Parameters

S-matrix reconstruction:				
f_0 = 352.1421 MHz	Q_0 = 6875		β = 1.1379	
$\beta_{1\ldots4}$ = 0.2679	0.2795	0.3123	0.2782	
(0.2693	0.2837	0.3107	0.2741 corrected)	
Multiport matching:				
f_0 = 352.1422 MHz	Q_0 = 6786		β = 1.1982	
$\beta_{1\ldots4}$ = 0.2797	0.2979	0.3218	0.2988	

Table 6: IPHI and Linac4 Operational Parameters

	$Q_{0\ realized}$	P_{Cu} kW	P_B kW	β_{ideal}	$\beta_{realized}$	Γ^2 dB
IPHI	6875	1170	300	1.26	1.14	–26
Linac4	6770	390	210	1.54	1.59	–36

CONCLUSION

The TLM approach has been successfully used for IPHI and Linac4 accurate tuning. Thermal stability of Linac4 has been experimentally demonstrated to be in close agreement with design.

REFERENCES

[1] O. Piquet et al., *RF Tuning of the IPHI RFQ*, THPME055, this Conference.

[2] C. Rossi et al., *Commissioning and operational experience gained with the Linac4 RFQ at the CERN Linac4*, LINAC'14, Geneva.

[3] O. Piquet et al., *RF design of the ESS RFQ*, THPPP031, IPAC'12.

[4] A.C. France et al., *Unsegmented vs. segmented 4-vane RFQ: theory and cold model experiments*, MOPD026, IPAC'10.

[5] A.C. France et al., *RF design and tuning of Linac4 RFQ*, WEPPC002, RuPac 2012.